Planetary and Space Science xxx (2017) 1–9

Contents lists available at ScienceDirect

Planetary and Space Science

journal homepage: www.elsevier.com/locate/pss

The scientific objectives and payloads of Chang'E−4 mission

Yingzhuo Jia [a,b,*], Yongliao Zou [a], Jinsong Ping [c], Changbin Xue [a], Jun Yan [c], Yuanming Ning [d]

[a] State Key Laboratory of Space Weather, National Space Science Center, Chinese Academy of Sciences, Beijing, 100190, China
[b] University of Chinese Academy of Sciences, Beijing, 100149, China
[c] National Astronomical Observatories, Chinese Academy of Sciences, Beijing, 100012, China
[d] Lunar Exploration and Aerospace Engineering Center, Beijing, 100028, China

ARTICLE INFO

Keywords:
Lunar exploration
Chang'E−4
Scientific objectives
Payloads

ABSTRACT

Chang'E−4 lunar explorer is the backup of the Chang'E−3, which is composed of a communication relay satellite, a lander and a rover, it is estimated that the Chang'E−4 explorer will be launched by the end of 2018, which is scheduled to land at the south pole Aitken Basin, and carry out the in situ detection and reconnaissance at the far side of the moon with the communication support of the relay satellite. Chang'E−4 mission has been planned to install six kinds of scientific payloads to complete the corresponding tasks, three kinds of payloads on the lander are the Landing Camera (LCAM), the Terrain Camera (TCAM), and the Low Frequency Spectrometer (LFS), and three kinds of payloads on the rover are the Panoramic Camera (PCAM), the Lunar Penetrating Radar (LPR), and the Visible and Near-Infrared Imaging Spectrometer (VNIS). The LFS is newly developed for Chang'E−4 lander, and other five kinds of payloads are the inherited instruments from Chang'E−3. Besides the above six payloads, there are also three international joint collaboration payloads to be installed on the Chang'E−4 explorer, which are the Lunar Lander Neutrons and Dosimetry(LND) installed on the lander, the Advanced Small Analyzer for Neutrals(ASAN) installed on the rover, Netherlands-China Low-Frequency Explorer (NCLE) installed on the relay satellite. The paper mainly discusses the Chang'E−4's scientific objectives, landing area overview, payloads configuration and system design, and the task for each payload with its main technology index.

1. Introduction

The Chinese Lunar Exploration Program (CLEP) is strategically divided into three phases as "Orbiting (Phase I), Landing (Phase II) and Sample Return (Phase III)". The Chang'E−4 mission is the backup mission for Chang'E−3, and composed of a communication relay satellite, a lander, and a rover. The relay satellite is newly developed, and will be at the Earth-Moon L2 Lagrange point, is estimated to be launched in June of 2018, with 3-year operation period in orbit. The lander and the rover have been developed after Chang'E−3, and are estimated to be launched in December of 2018. After 27-day flying, it will be operated and landed on the lunar far side. The landing site will be the South Pole Aitken basin (SPA). Chang'E−4 mission will perform the first lunar far side soft landing during the human history, and will perform the in-situ exploration and roving investigation.

Up to the scientific objectives and the relevant payloads of Chang'E−4 mission, the objectives and tasks of Chang'E−4 scientific mission have been formulated after conscientiously summing up the experiences and lessons of Chang'E−3 mission. They have been rearranged and modified from the backup of Chang'E−3 mission according to the new scientific goals, based on the new knowledge from the results of Chang'E−3 scientific exploration and investigation, and based on the existing resource and working condition, as well as based on balancing the scientific innovation and mission schedule. The CE-3 rover has a planned mission phase of three months, and the planned lander's mission phase is one year. Now they have obtained some science result. Fig. 1 is 360° stereo panoramas of lunar surface color panorama obtained by PCAM on the CE-3 Li et al., 2014), these millimeter to decimeter-resolution images are used to assist in the analysis of local morphological and structural characteristics. Extreme Ultraviolet Camera (EUVC) on the CE-3 on December 25, 2013 has been imaging the terrestrial plasmasphere in 30.4 nm wavelength during each lunar day, obtaining for the first time a lunar-based, wide-angle, continuous view of Earth's plasmasphere (Fig. 2) (Feng et al., 2014).

2. Scientific objectives

On the basis of the maximum utilization of Chang'E−3 technology

* Corresponding author. National Space Science Center, Chinese Academy of Sciences, Beijing, 100190, China.
E-mail address: jiayingzhuo@bao.ac.cn (Y. Jia).

https://doi.org/10.1016/j.pss.2018.02.011
Received 31 January 2017; Received in revised form 2 June 2017; Accepted 16 February 2018
Available online xxxx
0032-0633/

and products, the scientific objectives for Chang'E−4 mission have been finally chosen as: 1) low-frequency radio astronomical study on the lunar surface; 2) shallow structure investigation at the lunar far side of roving area; 3) the topographic and the mineralogical composition investigation for the lunar far side of roving area.

2.1. Low-frequency radio astronomical study on the lunar surface

Low-frequency radio astronomy in the frequency band below about 10 MHz cannot be done on the ground or be done well from space due to the Earth's ionosphere cut-off, man-made radio frequency interference (RFI), and the auroral kilometric radiation (AKR) noise. The lunar far side blocks the RFI, the AKR noise from the Earth. Additionally, it will also block the solar radio emission during the night time. Hence, the lunar far side has been believed as the best place for the low-frequency radio astronomical observation. Scientists from many nations are planning to do the low-frequency radio astronomical studies at the far side of the Moon.

To take the advantage of unique radio environment of lunar far side, the Chang'E−4 mission will investigate large scale characteristics of our Galaxy at low radio frequency, and create a new low-frequency high resolution map of the radio sky after long time survey. The mission will also carry out the first Earth-Moon space VLBI experiment at low radio frequency together with the ground low-frequency radio astronomical array. The mission will uncover the mechanism for the planetary low-frequency burst. The mission will offer great opportunity for studying the corona during solar radio bursts at frequencies below 30 MHz, with reasonable resolution at least for the bright events to follow coronal mass ejection (CMEs) out to 1 AU, to be used for improving the forecast in Space Weather. At the band from 100 KHz to 1 MHz, the mission will fill the gap in radio astronomical observation, so as to achieve original results at the directions of shock wave of solar wind, of CME and of creating mechanism for high energy electron beam.

The payload configuration and its exploration mission are using the LFS on the lander, and the NCLE on the relay satellite, to do joint low-frequency radio astronomical observation. Its specific exploration goals include: to obtain the map of radio sky at 2 frequencies at the band of 1 MHz–80 MHz, after 3-year operation, to investigate the earth AKR in the band of 0.1 MHz~1 MHz, to observe the Jovian radio emission at the band of 1 MHz–40 MHz, so as to test the power law hypothesis following with the planetary scale change of low frequency emission from planetary magnetosphere based on the observation result (Zarka, 2007), to observe and study the disastrous space weather events and the Type II & III solar burst at the band above 0.1 MHz, to do the Earth-Moon distance low frequency radio observation at the same time with a baseline of 4000 000 km at some special geometric configuration for the Moon, the Earth, the Sun and/or the Jupter, and to do 5–10 times initial Earth-Moon space VLBI with at least once successful experiment as the target.

2.2. Probing shallow structures of patrol area in moon's far side

There exists apparent difference in geological features between the nearside and far side of the Moon, the genesis of which is one of the major problems in the current Moon research. The SPA basin, 2500 km in diameter and 12 km in depth, is the oldest, largest and deepest impact crater. The huge impact crater likely exposed the deep lunar crust and probably the mantle materials, which is of essential significance to study the depth material of the Moon (Chikmachev et al., 2005). According to the Laser Altimeter data from Clementine Mission, it is apparent to identify three large circular structures in the northeastern basin. The inherent relationship between the shape feature and the formation and evolution of SPA is unknown, which deserves to be further simulated and argued according to the internal relationship between the impacting process and the shape structure feature.

The scientific payloads and its corresponding scientific exploration mission include probing the lunar regolith thickness and the shallow structure of the upper lunar crust with the LPR on the rover in patrol area, and exploring and studying the superficial structure of the special craters (Lai et al., 2016). The probing depth for the lunar regolith is more than 30 m with 30 cm vertical resolution. The probing depth for lunar crust is

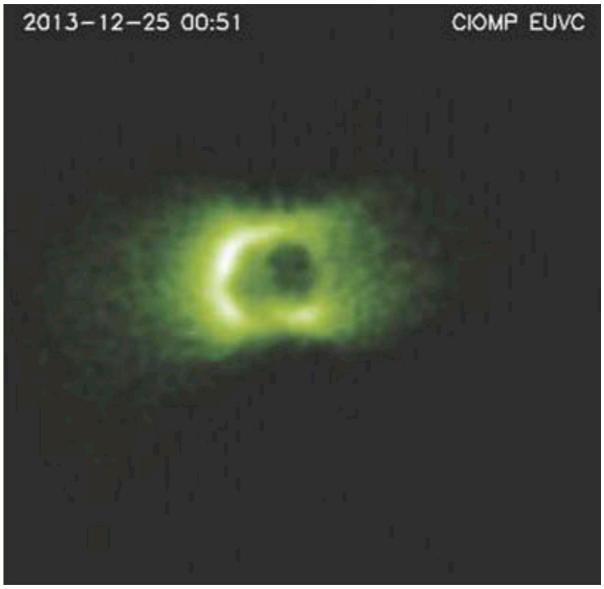

Fig. 2. Observation of Earth's plasmasphere by EUVC. The plasmasphere, plasmapause, airglow and Earth's shadow can be seen in this image.

Fig. 1. Lunar surface color panorama obtained by PCAM at exploration. In the background is the lander located to the northeast of the rover, with rover tracks between them visible on the ground. In the foreground are the two antennas of LPR.

more than 100 m with 10 m vertical resolution. Comparatively combining with the probing results from CE-3 mission, we may newly understand the detailed geologic evolutions about the lunar regolith and the Moon crust (Zhang et al., 2015). The analysis on the lunar shallow structure and its evolution can help to obtain the significant breakthrough about the evolution model and its theoretical system of the Moon.

2.3. Exploring morphology and mineral constituents of patrol area in moon's far side

The topography of lunar surface is not only a comprehensive manifestation of the surface evolution of the Moon, but also the direct object and product of the Moon contacted, subjected and impacted by the external materials. Probing the topography and mineral constituents of patrol area in Moon's far side is the indispensable basic information for the lunar scientific researches. The craters are the conspicuous geomorphic features of the lunar surface. The analysis of morphology, structure and spectral features of the typical craters will provide abundant information about cratering mechanism, impacting effects and evolutionary history. The SPA basin is selected as the landing site for CE-4 mission, which also took its unique material compositions and geological evolution into account.

The scientific payloads and its corresponding scientific exploration mission include LCAM and TCAM on the lander, and PCAM and VNIS on the rover, which is used to in-situ explore the lunar surface three-dimensional topography and the material components, especially to study the morphology and statistics of craters widely distributed in the area. Meanwhile, with the help of spectrum detection method, we can study the craters with the three-dimensional multi-spectrum method and obtain the three-dimensional geometrical morphology of craters and the distribution and its profile structure of the crater ejecta, etc. Spectral range of the infrared imaging spectrometer covers visible to near infrared wavelengths, which can be used to identify pyroxene, olivine and plagioclase and other rock-forming minerals according to the absorption features of such silicate minerals in this range (Ling et al., 2015). Remote sensing detection in global scale have found the region has rich mafic materials, so that such ultramafic rocks as norite and allivalite can likely be found during the patrolling exploration. These rock samples will be important to study components of lunar crust and mantle, to reveal unique geological evolution history in this region, and to analyze early evolution of the Moon. The Chang'E−4's mission will combine a variety of detection means, which is used to firstly establish a comprehensive geological profile integrated topography, geological structure, material composition and shallow structures of Moon's far side, and to establish the evolution model of regional geochemistry and tectonic dynamics.

3. Introduction of landing area

According to the general requirement of the Chang'E−4 project, Key Laboratory of Lunar and Deep Space Exploration at Chinese Academy of Sciences and the fifth department of Chinese Academy of Space Technology jointed for carrying out the selection of the landing site. Mainly aiming at scientific objectives and engineering capacity, on the premise of security, the landing site selection is of value in scientific research, also in such aspects as topography and communication satisfying the engineering requirement. The original range was selected as 30°–55°S or 30°–55°N in latitude and 110°–180°E or 110°–180°W in longitude. And the coverage is not less than 2° along latitude and 14° along longitude. Analyzing by digital elevation model (DEM) in spatial resolution of 500 m, the area of the region with the slope less than 8° should be no less than 60 percent of the whole coverage. Using the DEM data and slope data with spatial resolution of 500 m, Key Laboratory of Lunar and Deep Space Exploration chose 9 areas for potential landing sites, there are four in the northern hemisphere (N1∼N4) and five(S1∼S5) in southern hemisphere (Fig. 3).

The SPA basin (S5) is considered to be most suitable for landing area. Firstly, there will be detailed analysis of the geological morphological features and elevation profiles for the 9 alternative landing sites. Secondly, the correlative significances of scientific exploration, such as the distribution of lunar dust and geomagnetic remanence, temperature and particle radiation, local geochemistry, tectonic dynamics and internal layered structures and radio astronomy in low frequencies, were taken into deep analysis. Finally, the critic comparisons were made for the alternative landing sites in the reliability of the scientific objects.

S5 is located in 45° S to 55° S and 162° W to 144° W. The local maximum elevation difference is up to 6518 m, and 81.53 percent of the region has the slope less than 8°. Nectarian Plain is the main base material of exposed area with several ancient craters formed in Nectarian era or pre-nectarian era (Wilhelms and Wilshi, 1979; Wood and Gifford, 1980). Obviously, the preliminary selected landing site is within SPA basin with ancient craters, which makes the site be a suitable place to study the age, materials composition, and formation mechanism of the craters of the same kind. There exist abundant later overlaid craters or basins in SPA basin floor, the accumulated materials may not only originate from the impacting process during the crater formation, but also has the eject from the SPA event, e.g Nectarian Ingenii crater and pre-Nectarian Apollo basin both have the eject brought by SPA impacting (Petro and Pieters, 2004; Pieters et al., 2001). As a consequence, research of the craters or basins in the SPA basin is significant to understand the experienced impact events from Pre-Nectarian era to Imbrian era, which provides a basis to separate the terrane tectonic structure and geologic time.

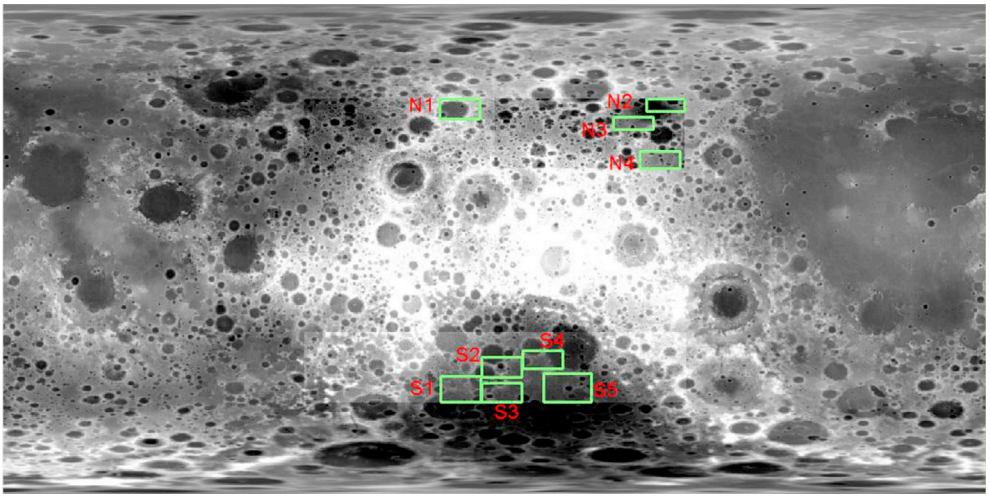

Fig. 3. The distribution of the alternative landing sites for CHANG'E−4 mission(N1: 55°–48°N, 160°–175°E; N2: 55°–51°N, 110°–124.5°W; N3: 48°–44°N, 122°–136°W; N4: 30°–36°N, 112°–127°W; S1: 46°–55°S, 160°–175°E; S2: 39°–46°S, 175°N∼170°W; S3: 48°–55°S, 175°N∼170°W; S4: 36°–43°S, 170°–155°W; S5: 45°–55°S, 162°–144°W).

The SPA basin is the largest and oldest impact basin of the Moon (Spudis et al., 1994). Although the terrain is low, the region are not filled with mare basalts as other Moon basins, suggesting its special thermal history and unique evolution features. The materials in the region are rich in mafic (Lin, 2010), which is likely to be of great significance to reveal the compositions of the crust and even the mantle of the Moon. All kinds of lunar exploration data show that SPA basin possesses unique geochemical characteristics. The Fe, Ti and Th abundances are higher in SPA basin, and FeO and TiO2 abundances here are abnormally high over the Moon farside. The FeO abundance in the basin is 7% higher than that in the surrounding regions. The TiO2 abundance is increased in some places of the basin where the Th and K abundances are also relatively high (Peterson et al., 2000, 2002). The rocks in SPA basin are dominated by plagioclase and norite, and basalt and troctolite are rare (Pieters et al., 2001). The anorthosite material is mainly distributed in Apollo crater, Ingenii crater and the Poincare basin at the SPA basin. For the terrain of SPA basin is low, the lunar crust here should be thin, and there should theoretically exist abundant mare basalts. The current data discovered mare materials in some craters, and the study on the mare basalt contents may provide some important signatures for the lunar geothermal evolution and earlier differentiation process.

4. Configuration and design of the scientific payloads

4.1. Design of the scientific payloads

The TCAM, LCAM and LFS were chosen as the scientific payloads for CE-4 lander, while the rover was equipped with several other three scientific payloads including the PCAM, LPR and VNIS. The lander and rover each had a payload controller which was designed to process, storage and control the scientific payloads data and allot tasks to payloads sensor heads. Each payloads sensor head had its own detector circuit board, which was inserted in the payloads controller. Each controller had a high performance central processing unit (CPU) and several distributed field programmable gate arrays (FPGAs) architecture, which were used to achieve the controlling needs of the scientific payloads. The payloads controllers also converted +28 V bus voltage to +5 V, ±15 V,+3.3 V secondary power supply voltage for ach payloads sensor head, and monitored the voltages and the temperatures (Jia et al., 2014; Dai et al., 2014). The scientific payloads system composition of the lander and the rover including the interface among the internal parts, the interface between the payloads controller and each payload sensor head are shown in Fig. 4 and Fig. 5.

There are 6 circuit boards embedded in the payload controller of the lander, three of them are the circuit boards of the payloads, and the rest are the circuit board that are used to systematically process, control and storage data for the scientific payloads system of the lander. Function of the payload controller includes: the first is to supply electric power for the payloads, the second is to set a schema of data caching space for buffering the data in preprocessing, the third is to connect the data manager of the rover via 1553B bus and low-voltage differential signaling(LVDS) bus in order to transmit scientific payloads data. The payloads of the lander connectted to the payload controller by 422 bus and LVDS bus that transmit controlling signal and scientific exploration data. The heart of the controller was an ATMEL AT697F microprocessor. The block of 256 MB SDRAM provided storage for the data and program. 512KBytes EEPROM copied at least one flight code and held the bootstrap code that operated the instrument. The FPGAs, namely XQR2V3000-4CCG717, received the data from the payloads sensor heads, and provided UARTs for communications with the CPU. Because the scientific payloads must work for a long period contact, we had implemented a watchdog timer that could protect them in case of an anomaly. This timer monitored processor activity status, if processor wasn't active for 5s, it would reset the microprocessor, and set a status bit that could be read on start-up. In order to had sufficient radiation capability, some parts were shielded in the scientific payloads controller with a minimum wall thickness of 0.38 cm of aluminum, which reduced the expected radiation dose to safety level.

There are 6 circuit boards embedded in the payload controller of the rover, three of them being used for the processing, controlling and storing the data for the scientific payloads system of the rover, the rest being controller board of circuit board for LPR, VNIS and PCAM. The payloads of the rover connect the data manager of the rover via 422 bus and LVDS bus, transmitting controlling signals and scientific exploration data. The payload controller of the rover adopts 80C32 data processing unit, stores scientific data using 256M SDRAM, controls and receives the scientific payloads data via 6 FPGA of model XQR2V3000-4CCG717.

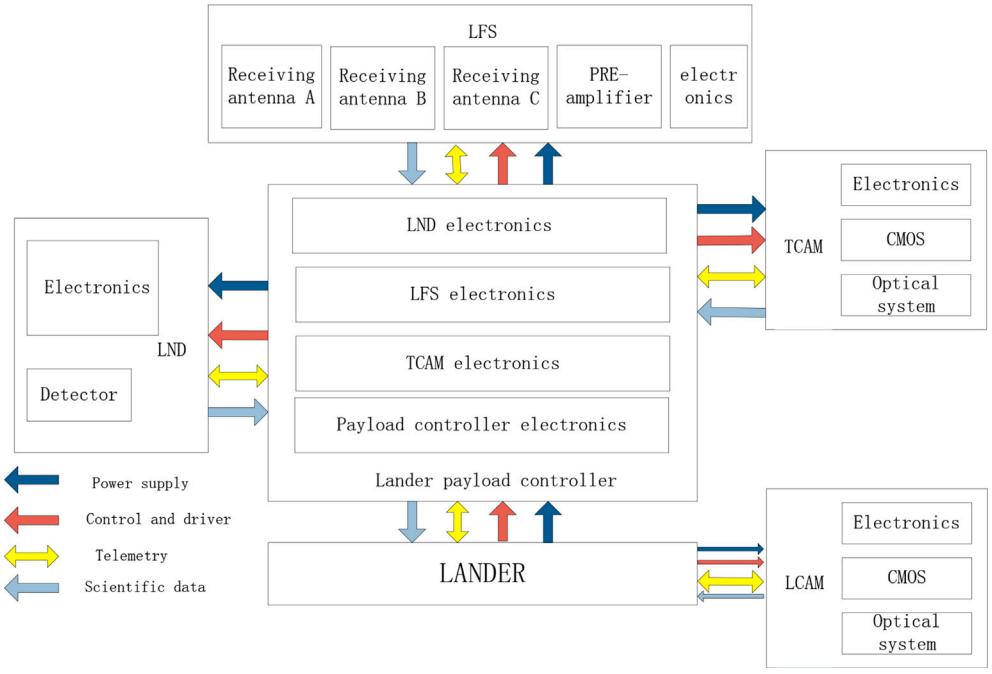

Fig. 4. Scientific payloads system for the Lander of Chang'E−4 mission.

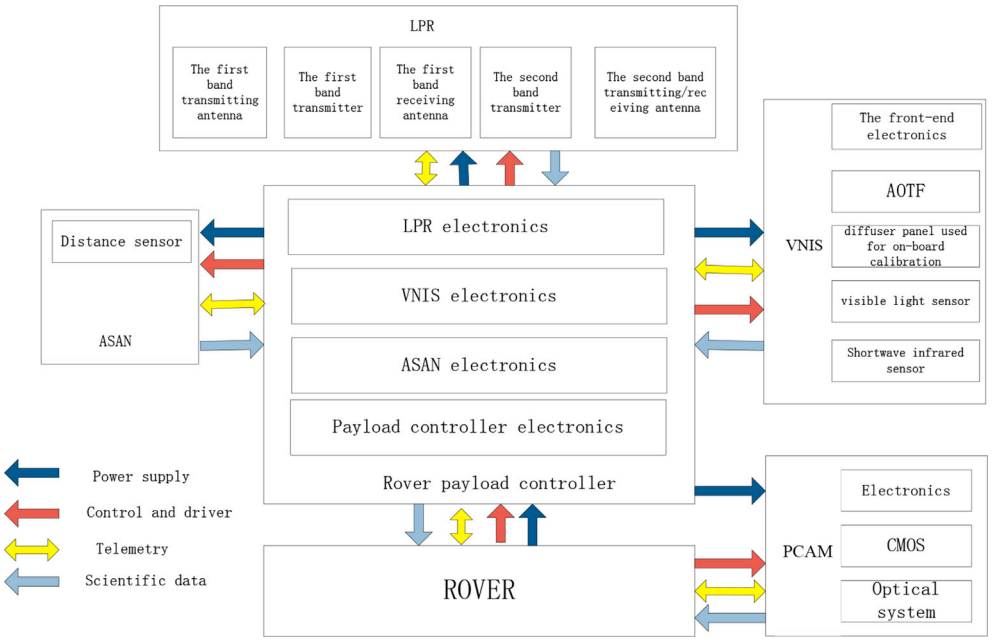

Fig. 5. Scientific payloads system for the Rover of Chang'E−4 mission.

4.2. Design detail of individual instruments

4.2.1. Landing camera

LCAM is mounted on the bottom of the CE-4 spacecraft, and the optical axis points in the +Z direction (toward the lunar ground in the most process of descent). LCAM is made up of the optical system, the mechanical system and the electronics control units and used complementary metal oxide semiconductor (CMOS) image sensor as a detector. The camera took video during the CE-4 spacecraft's descent toward the lunar surface. The camera took 1024 × 1024 pixel images at ~10 frames per second throughout the period of working time. At the height of 12 km above the lunar surface, the camera began to produce a video stream of high-resolution, overhead views of the landing site. It continued acquiring images until the spacecraft landed. But there are horizontal and vertical motions in the process of camera descent which would influence the image quality in the integral time. So the shorter exposure time would be used in LCAM for improving precision. During the camera exposure time, the lander's horizontal velocity result to camera's pixel remove less than 0.5 pixel, and corresponding to the reduce of the modulation transfer function (MTF) is less than 0.9 and the effect of vertical on the object is better than 0.72% (Jia et al., 2014; Dai et al., 2014). The total weight of the LCAM is 0.5 kg, and the body size is 116 × 100 × 70.4(mm). The composition diagram of LCAM is shown in Fig. 6, and the main performance of LCAM are shown in Table 1.

4.2.2. Terrain camera

The terrain camera is a high-resolution color CMOS cameras used to image the lunar surface and the rover. The camera is located on a camera bar that sits on top of the Lander. The camera bar allows the camera to

Table 1
Main performance of Landing Camera.

Number	Items	Parameters
1	Spectral range(nm)	419–777
2	Normal imaging distance(m)	4 ~ ∞
3	Effective pixel numbers	≥1024 × 1024
4	Field of view(°)	45 × 45
5	Optical system static MTF	≥0.20
6	Signal to noise ratio S/N (dB)	40(Maximum signal-to-noise ration) 30 (Albedo is 0.09, Incidence angle of the Sun is 30°)

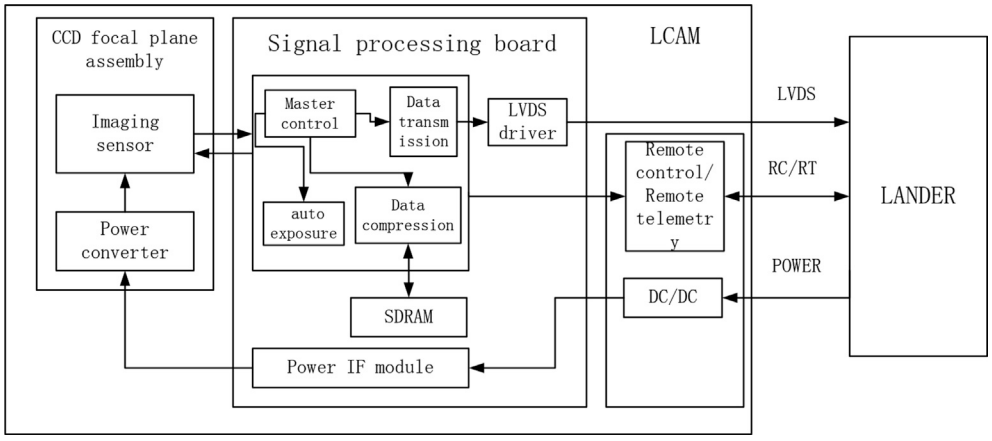

Fig. 6. Composition diagram of LCAM.

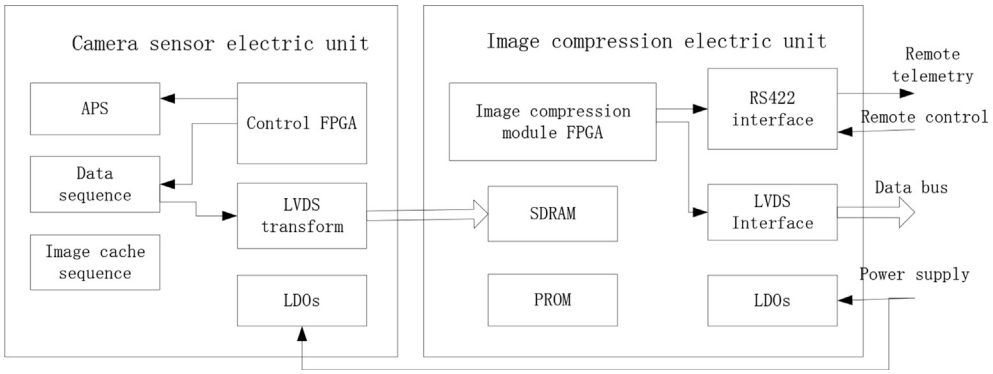

Fig. 7. Composition diagram of the terrain camera.

Table 2
The main performance of Terrain Camera.

Number	Items	Parameters
1	Spectral range(nm)	420–700
2	Color	R, G, B
3	Normal imaging distance(m)	5~∞
4	Effective pixel number	≥2352 × 1728
5	Field of view(°)	22.9° × 16.9°(≤5%)
6	Signal to noise ratio S/N(dB)	40(Maximum signal-to noise ration) 30 (Albedo is 0.09, Incidence angle of the Sun is 30°)
7	Optical system static MTF	≥0.20

rotate a full 360° to obtain a panoramic view of the lunar surface landscape. The camera bar itself can swing up or down through 120° of elevation. Scientists use the camera to create a map of the area where the CE-3 lander lands, as well as search for interesting rocks and soils to study. Engineers are more interested in observing the rover. Engineers use instrument to image how the rover conducts science investigation on the lunar surface, such as how Pancam Mast rises from the deck and how turns the cameras in the horizontal plane and vertical plane, how the rover swerve and curve, how the rover arm maneuvers the instruments to get up-close the rocks and soil (Jia et al., 2014; Dai et al., 2014). The total weight of the TCAM is 0.64 kg, and the body size is 92 × 105 × 118.9(mm). Terrain camera system is shown in Fig. 7. The main performance is shown in Table 2.

4.2.3. The low-frequency radio spectrometer

The scientific objectives of the LFS is to investigate the low frequency electrical field generated by solar burst and to study the lunar ionosphere. In order to server this purpose, the LFS is developed to detect the low frequency electrical field from the sun, interplanetary space and galactic space, etc. Based on the variety of the low frequency electric field, the characteristics of the ionospheric environment over the landing area will be studied.

In the LFS, the tricomponent active antenna element will be used to receive the electromagnetic wave from the sun and the space. The three mutually perpendicular components of the electromagnetic wave will be received respectively. According to the theory of radio wave propagation, we can get the intensity, spectrum, time variation, polarization of low frequency electromagnetic wave and the direction of radiation source by the analysis of the three component data (Chen et al., 2010). The low-frequency radio spectrum consists of electric unit, preamplifier, three receiving antenna, cable assembly. The electric unit comprises a

Table 3
The main performance of Low-frequency radio spectrometer.

Number	Items	Parameters
	bandwidth	0.1–40 MHz
2	Receiver sensitivity	≤10nV/ $\sqrt{Hz}$
3	Dynamic range	≥75 dB
4	Frequency resolution	1 ~ 10KHz (0.1 ~ 1.0 MHz) 100 ~ 200 kHz (1.0 ~ 40 MHz)

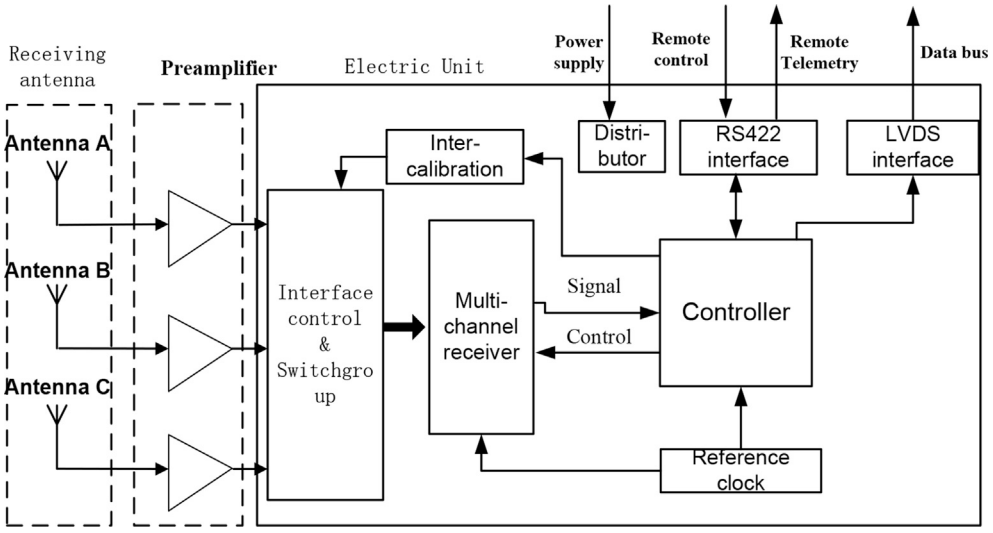

Fig. 8. Composition of the Low-frequency radio spectrometer system.

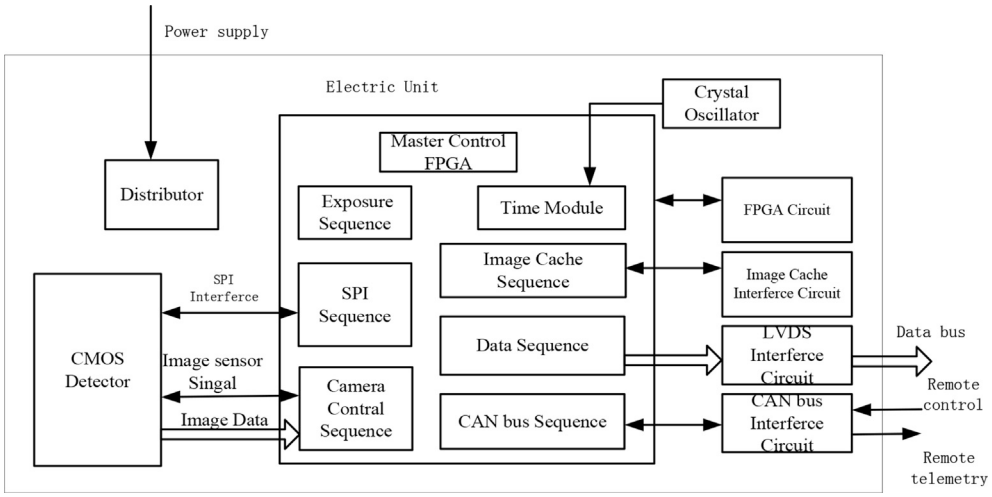

Fig. 9. Composition diagram of the panoramic camera.

Table 4
The main performance of the Panoramic Camera.

Number	Items	Parameters
1	Spectral range(nm)	420–700
2	Image mode	Color mode; Panchromatic mode (Can be switched)
3	Normal imaging distance(m)	3 ~ ∞
4	Field of view(°)	19.7 × 14.5
5	Signal to noise ratio S/N (dB)	40(Maximum signal-to noise ration) 30 (Albedo is 0.09, Incidence angle of the Sun is 30°)
6	Optical system static MTF	≥0.20

controller, a distributor and a reference clock module, multi-channel receiver, inter-calibration module, communication interface, data transmission interface group. The receiving antenna and the preamplifier are arranged outside the lander cabin, and the electric unit is arranged in the lander cabin. The diagram of LFS is shown in Fig. 8. The main performance is shown in Table 3.

4.2.4. Panoramic camera

PCAM is composed of two cameras with identical functions, performances and interfaces, and is installed on the lunar rover mast. The mast allows the cameras to rotate a full 360° to obtain a panoramic view. It can acquire 3D images of the lunar surface based on the principle of binocular stereovision. Combined with integration design PCAM is made up of the optical system, the mechanical system, the electronics and thermal control units. The camera also has the ability to take color and panchromatic images with 19.6° × 14.5°FOV. It used a Bayer color filter array covering CMOS sensor to capture color images. RGB values of the original images are related to the camera. The standards which were published by the international commission on illumination were used to establish a color correction model, and the color correction coefficient will be obtained (Dai et al., 2014; Wu et al., 2014). The total weight of the PCAM is 0.69 kg, and the body size is 90 × 110 × 120(mm). The composition diagram of PCAM is shown in Fig. 9, and the main performance of PCAM is shown in Table 4.

4.2.5. Lunar penetrating radar

The scientific objective of the LPR is to detect the lunar subsurface structure on the patrol route, and to detect the thickness and structure of the lunar regolith. LPR will be start up when the rover moves. During these periods, in order to balance the detection depth and resolution, two detection channels will be used. LPR is nanosecond impulse radar with bistatic antennas which works in the time domain. The main scientific objective is to detect the structure of lunar subsurface and lunar regolith on the patrol route. Ultra-wideband nanosecond impulse is produced by the transmitter, sent through the transmitting antenna down to lunar surface. The receiving antenna receives the reflected signal. The echo signal from the underground target is received by the receiving antenna, amplified in the receiver and then restored as data record. The two work frequency bands of LPR are 40–80 MHz and 250–750 MHz (Fang et al.,

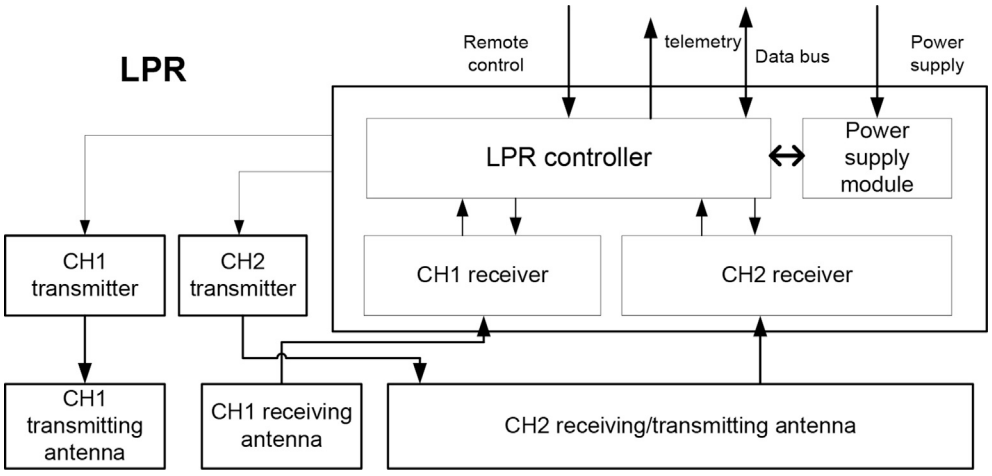

Fig. 10. Composition of the LPR system.

Table 5
The main performance of LPR.

Number	Items		Parameters	
			CH1	CH2
1	Transmitter	Pulse amplitude(V)	1000(with 5% bias)	≥400(with 5% bias)
2		Pulse repetition frequency(kHz)	0.5,1,2(Switchable)	5,10,20(Switchable)
3		Pulse Rising time(ns)	≤5	≤1
4	Receiver	Receiver band(MHz)	10–175	10–1000
5		Receiver dynamic range(dB)	Better than 90	Better than 90
6	The Tx Antenna and Rx Antenna	Central frequency(MHz)	60	500
7		Antenna band(MHz)	≥40	≥450
8		Voltage Standing Wave Ratio	≤3	≤2.5
9	The penetrating-depth(m)		≥100	≥30
10	The thickness resolution		meter magnitude	≤30 cm

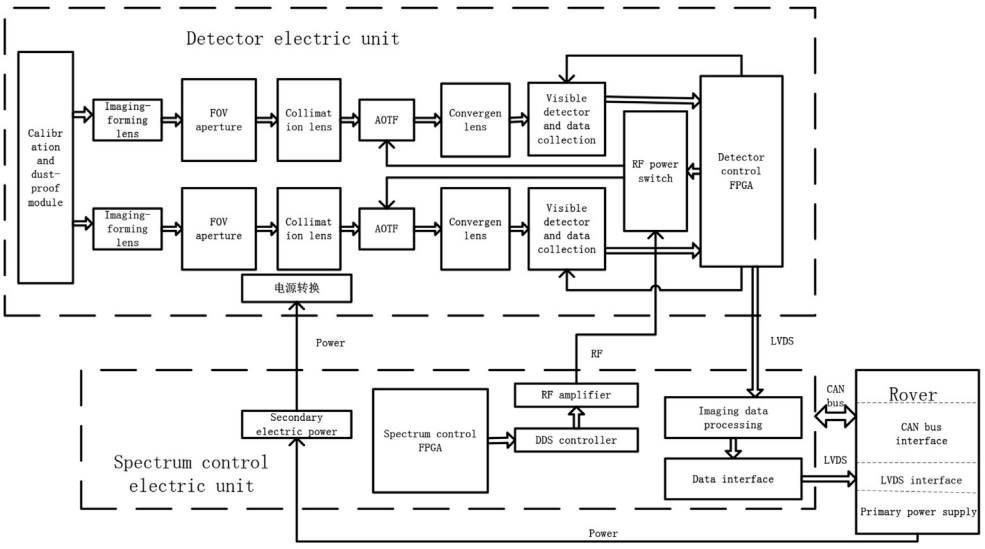

Fig. 11. System design of VNIS.

2014). The LPR system is shown in Fig. 10. The main performance of LPR is shown in Table 5.

4.2.6. Infrared imaging spectrometer

The primary mission of VNIS is to acquire the visible spectral image and infrared spectral curve around the patrol area for the analysis of lunar surface mineral constituent and distribution. The VINS consists of sensor, cable assemblies and electronics units. Sensor consists of front optical assemblies, acousto-optic tunable filter, convergent mirror and sensor assemblies. Electronics unit consists of visible and shortwave sensor driver and drivers of signal acquisition, thermoelectric cooling, and radio frequency power amplifier, acousto-optic turnable filter (AOTF) amplifier switch, spectral detection control, secondary power supply and dust proof machine. The two optical channels are visible channel and infrared channel, whose detection band ranges from 0.4 μm to 2.4 μm. The two channels are converted by the AOTF (He et al., 2014). AOTF is a narrow-band tunable filter and it is a kind of light dispersion device based on the acousto-optic interaction principle. The wavelength of the monochromatic light will be changed accordingly when the crystal frequency is changed. The total weight of the VNIS is 4.69 kg, and the body size is 255 × 172 × 162(mm). The components of VNIS are shown in Fig. 11 and the main performance is shown in Table 6.

Table 6
The main performance of Infrared Imaging Spectrometer.

Number	Items	Visible near-infrared channel	Near-infrared short-wave infrared channel
1	Band range(nm)	450 ~ 950	900 ~ 2400
2	Spectral resolution(nm)	2 ~ 10	3 ~ 12
3	Field of view(°)	≥6 × 6	≥2 × 2
4	Effective pixel count	256 × 256	1
5	System static transfer function MTF	>0.1	/
6	Signal to noise ratio S/N(dB)	≥40(Maximum) ≥30(Albedo 0.09, Incidence angle of the sun is 45°)	≥40(Maximum) ≥30(Albedo 0.09, Incidence angle of the sun is 15°)

5. International cooperation payloads

Chang'E−4 mission will carry three international collaboration payloads, which include the Lunar Lander Neutrons and Dosimetry(LND) on the lander and the Advanced Small Analyzer for Neutrals(ASAN) on the rover, and the Netherlands-China Low-Frequency Explorer(NCLE) on the relay communication satellite. The three international collaboration payloads have good technical maturity and product inheritance, by means of foreign oriented research and development. The foreign partners will have their own intellectual property rights for autonomous technologies. According to work needs, the Chinese and foreign parties will clear the interface parts in the form of interface control documents. About the scientific data and results obtained by the relevant payload, the Chinese and foreign parties will share these achievements. This paper simply descript the international collaboration payloads. The scientific objectives and the Principle Investigator(PI) for each of them is listed in

Table 7
Scientific objectives for the international collaboration payloads.

Payload Name	Scientific Objectives/Exploration Task	Foreign Party	Chinese PI Party	S/C
Lunar Lander Neutrons and Dosimetry(LND)	To Measure the lunar surface integrated particle radiation dose and the LET spectra, to measure the lunar surface fast neutron spectrum and thermal neutron spectrum.	University of Kiel, Germany	National Space Science Center, Chinese Academy of Sciences	Lander
The Advanced Small Analyzer for Neutrals(ASAN)	To study the memory mechanism of lunar surface sputtering process of the lunar atmosphere, to measure in-suit at the surface the energetic neutral atom fluxes backscattered from the lunar surface.	Institute of space physics, Sweden	National Space Science Center, Chinese Academy of Sciences	Rover
Netherlands-China Low-Frequency Explorer (NCLE)	To map the radio sky at low frequency band for studying the large scale of the Galaxy, to detect and explore the solar radio burst and planetary radio bursts.	Radboud University Nijmegen, Netherland	National Astronomical Observatories, Chinese Academy of Science	Relay S/C

The LND performance requirements is given in Table 8, the ASAN performance requirements is given in Table 9, the performance requirements of NCLE is given in Table 10.

Table 8
The Lunar Lander Neutrons and Dosimetry performance requirements.

Items	Parameters
Fast neutron spectrum	2-20 MeV, 32 channels
Thermal neutron flux	10-104/min
Proton energy spectrum	7-30 MeV, 32 channels
electron spectroscopy	60-500 keV, 32 channels
Alpha particle energy spectrum	7-20MeV/n, 32 channels
Heavy ion energy spectrum	10-30MeV/n,32 × 32 matrixes
LET spectral range	0.1–430 keV/μm, 64 energy channels
Time resolution	dose rate: 1 min; proton: 5 min electron: 5 min; heavy ion: 30 min

Table 9
The Advanced Small Analyzer for Neutrals performance requirements.

Items	Parameters
observation element	Energy neutral atom(ENA), positive ion
energy range	10eV–10 keV
mass resolution	Energy neutral atom:hydrogen atom, other constituent groups positive ion:mass charge ratio 1,2,4,8,16,32
energy resolution	7%(positive ion),30%(Energy neutral atom)
Time resolution	10s

Table 10
Netherlands-China Low-Frequency Explorer performance requirements.

Items	Parameters
Work frequency/spectral resolution	100 kHz~1MHz/1 kHz 1 MHz–10 MHz/10 kHz 10 MHz–80 MHz/100 kHz
Crystal time stability	$<5 \times 10^{-11}$(short time stability)
Receiver sensibility	<-160 dBm/Hz@10 MHz
Dynamic range	≥84 dB
Space interferometric baseline	>400000 km
Interference angle resolution	≤1 Mbps

Table 7.

6. Conclusion

In order to implement the scientific objectives and make maximum utilization of Chang'E−3, the Chang'E−4 payload configuration scheme is proposed. Generally, CE-4 will be the first times in the world to have Lunar landing and roving on the far side, hence the lunar scientific exploratory data obtained by the payloads will be the first hand data source in the world, and the moon science achievements based on the above data source will be taken as "the original" results. By the joint teamwork of combining these payloads on the lander and rover together, integrated geological section profile will be constructed based on the analysis of moon topography, geological structure, material composition and shallow structure. It will also be the first time work in the world. Meanwhile, Low frequency radio astronomical observation can also fill a gap in the astronomical world, which has a very high originality.

Acknowledge

This work was supported by National Natural Science Foundation of China under Grant No.41590851.

Appendix A. Supplementary data

Supplementary data related to this article can be found at https://doi.org/10.1016/j.pss.2018.02.011.

References

Chen, Linjie, Amin, Aminali, Yan, Yihua, 2010. Characteristics analysis of tripole antenna for lunar very low frequency interferometer. Chin. J. Radio Sci. 06, 1064–1072.
Chikmachev, V.I., Pugacheva, S.G., Shevchenko, V.V., 2005. General Structure of the Lunar South Pole-aitken Basin and Possible Genesis of it [C]//Lunar and Planetary Science, XXXVI: Papers Presented to the Thirty-sixth Lunar and Planetary Science Conference. Lunar and Planetary Science Conference, Houston, p. 1078.
Dai, Shuwu, Jing, Yingzhuo, Zhang, Baoming, et al., 2014. Chang'E-3 scientific payloads and its checkout results. Sci. Sin. Tech. 44 (4), 361–368 (In Chinese).
Fang, Guangyou, Zhou, Bin, Ji, Yicai, et al., 2014. Lunar Penetrating Radar Onboard the Chang'e-3 Mission. Res. Astron. Astrophys. 14, 1607.
Feng, J.Q., et al., 2014. Data processing and initial results from the CE-3 extreme ultraviolet camera. Res. Astron. Astrophys. 14, 1674–1681.
He, Zhiping, Wang, Binyong, Lv, Gang, et al., 2014. Operating principles and detection characteristics of the Visible and Near-Infrared Imaging Spectrometer in the Chang'e-3. Res. Astron. Astrophys. 14, 1567–1577.
Jia, Yingzhuo, Dai, Shuwu, Wu, Ji, et al., 2014. Chang'E-3 lander's scientific payloads. Chin. J. Space Sci. 34 (2), 219–225 (In Chinese).
Lai, Jialong, Xu, Yi, Zhang, Xiaoping, et al., 2016. Structural analysis of lunar subsurface with Chang'E-3 lunar penetrating radar. Planet. Space Sci. 120 (2016), 96–102.
Li, Chun-Lai, Mu, Ling-Li, Zou, Xiao-Duan, et al., 2014. Analysis of the geomorphology surrounding the Chang'e-3 landing site. Res. Astron. Astrophys. 14, 1514.
Lin, Yangting, 2010. Key issues of the formation and evolution of the Moon. Geoch.China 39 (1), 1–10 (in Chinese).
Ling, Zongcheng, Jolliff, Bradley L., Wang, Alian, et al., 2015. Correlated compositional and mineralogical investigations at the Chang'e-3 landing site. Nat. Commun. 6.
Peterson, C.A., Hawke, B.R., Lucey, P.G., Taylor, G.J., Blewett, D.T., Spudis, P.D., 2000. Anorthositeon the Lunar Farside and its Relationship to South Pole-aitken Basin. Lunar and planetary Science XXXI, pp. 1680–1681.
Peterson, B.R.H.C.A., Blewett, D.T., Bussey, D.B.J., Lucey, P.G., Taylor, G.J., Spudis, P.D., 2002. Geochemical units on the moon: the role of south pole-aitken basin. Lunar and Planetary Science XXXIII 46–47.
Petro, N.E., Pieters, C.M., 2004. Surviving the heavy bombardment: ancient material at the surface of south pole-aitken basin. J. Geophys. Res. 109, 1–13.
Pieters, C.M., Gaddis, L., Jolliff, B., Duke, M., 2001. Rock types of south pole-aitken basin and extent of basaltic volcanism. J. Geophys. Res. 106, 28001–28022.
Spudis, P.D., Reisse, R.A., Gillis, J.J., 1994. Ancient multiring basins on the moon revealed by clementine laser altimetry. Science 266, 1848–1851.
Wilhelms, D.E.K.A.H., Wilshi, H.G., 1979. Geologic map of the south side of the moon, Scale 1:5000000. U. S. Geol. Surv., Map 1–1162.
Wood, C.A., Gifford, A.W., 1980. Evidence for the lunar big back side basin. LPI Contrib. 414, 121–123.
Wu, Fanlu, Liu, Jianjun, Ren, Xin, Li, Chunlai, 2014. Research on panoramic method of Chang'e-3 pancam images. Acta Opt. Sin. 09, 182–190.
Zarka, Philippe, 2007. Plasma interactions of exoplanets with their parent star and associated radio emissions. Planet. Space Sci. 55, 598–617.
Zhang, Jinhai, Yang, Wei, Hu, Sen, Lin, Yangting, Fang, Guangyou, et al., April 28, 2015. 2015, Volcanic history of the Imbrium basin: a close-up view from the lunar rover Yutu. Proc. Natl. Acad. Sci. Unit. States Am. 112 (17), 5342–5347.